AMERICAN SOCIETY FOR MICROBIOLOGY | Applied and Environmental Microbiology®

BIODEGRADATION

Filling in the Gaps in Metformin Biodegradation: a New Enzyme and a Metabolic Pathway for Guanylurea

Lambros J. Tassoulas,[a] Ashley Robinson,[a] Betsy Martinez-Vaz,[a] Kelly G. Aukema,[a] Lawrence P. Wackett[a]

[a]Department of Biochemistry, University of Minnesota, Saint Paul, Minnesota, USA

Lambros J. Tassoulas and Ashley Robinson contributed equally to the manuscript. Author order was selected based upon mutual agreement.

ABSTRACT The widely prescribed pharmaceutical metformin and its main metabolite, guanylurea, are currently two of the most common contaminants in surface and wastewater. Guanylurea often accumulates and is poorly, if at all, biodegraded in wastewater treatment plants. This study describes *Pseudomonas mendocina* strain GU, isolated from a municipal wastewater treatment plant, using guanylurea as its sole nitrogen source. The genome was sequenced with 36-fold coverage and mined to identify guanylurea degradation genes. The gene encoding the enzyme initiating guanylurea metabolism was expressed, and the enzyme was purified and characterized. Guanylurea hydrolase, a newly described enzyme, was shown to transform guanylurea to one equivalent (each) of ammonia and guanidine. Guanidine also supports growth as a sole nitrogen source. Cell yields from growth on limiting concentrations of guanylurea revealed that metabolism releases all four nitrogen atoms. Genes encoding complete metabolic transformation were identified bioinformatically, defining the pathway as follows: guanylurea to guanidine to carboxyguanidine to allophanate to ammonia and carbon dioxide. The first enzyme, guanylurea hydrolase, is a member of the isochorismatase-like hydrolase protein family, which includes biuret hydrolase and triuret hydrolase. Although homologs, the three enzymes show distinct substrate specificities. Pairwise sequence comparisons and the use of sequence similarity networks allowed fine structure discrimination between the three homologous enzymes and provided insights into the evolutionary origins of guanylurea hydrolase.

IMPORTANCE Metformin is a pharmaceutical most prescribed for type 2 diabetes and is now being examined for potential benefits to COVID-19 patients. People taking the drug pass it largely unchanged, and it subsequently enters wastewater treatment plants. Metformin has been known to be metabolized to guanylurea. The levels of guanylurea often exceed that of metformin, leading to the former being considered a "dead-end" metabolite. Metformin and guanylurea are water pollutants of emerging concern, as they persist to reach nontarget aquatic life and humans, the latter if it remains in treated water. The present study has identified a *Pseudomonas mendocina* strain that completely degrades guanylurea. The genome was sequenced, and the genes involved in guanylurea metabolism were identified in three widely separated genomic regions. This knowledge advances the idea that guanylurea is not a dead-end product and will allow for bioinformatic identification of the relevant genes in wastewater treatment plant microbiomes and other environments subjected to metagenomic sequencing.

KEYWORDS guanylurea hydrolase, metformin, *Pseudomonas mendocina*, biodegradation, enzyme, genome, guanidine, CgdAB

Guanylurea (carbamylguanidine) is one of the most widespread water contaminants, originating and accumulating from metformin, a first-line globally important drug (1, 2). Metformin is widely prescribed as a treatment for type 2 diabetes and

Citation Tassoulas LJ, Robinson A, Martinez-Vaz B, Aukema KG, Wackett LP. 2021. Filling in the gaps in metformin biodegradation: a new enzyme and a metabolic pathway for guanylurea. Appl Environ Microbiol 87: e03003-20. https://doi.org/10.1128/AEM.03003-20.

Editor Hideaki Nojiri, University of Tokyo

Address correspondence to Lawrence P. Wackett, wacke003@umn.edu.

Received 10 December 2020
Accepted 10 March 2021
Accepted manuscript posted online 19 March 2021
Published 11 May 2021

has even heightened significance in light of its observed anti-inflammatory, anticancer, and antiaging effects (3–6). Most recently, metformin has been associated with reduced mortality in COVID-19 patients suffering from preexisting conditions such as diabetes and obesity (7). Those studies also showed that human drug-metabolizing enzymes do not transform metformin, the drug is largely excreted unchanged, and microbes in wastewater treatment plants and aquatic environments transform it to guanylurea.

Guanylurea has been widely labeled as a recalcitrant "dead-end" product of metformin in numerous wastewater treatment systems (8, 9). Guanylurea forms, and has been detected in, wastewater treatment plant effluent and coastal waters around the globe (4, 10–12). Metformin and guanylurea have been reported in surface waters at levels of micrograms per liter, which is extremely high for a pharmaceutical contaminant (12, 13). Metformin was detected in European surface waters at levels of up to 3 μg/liter, with guanylurea concentrations exceeding those of metformin by an order of magnitude or more (14–16).

It is also relevant that metformin and guanylurea are charged molecules that bind poorly to granulated activated carbon, the worldwide standard treatment for removing pharmaceuticals, which are largely hydrophobic molecules (12, 17). In that context, biodegradation is even more crucial for their removal. The levels of these compounds entering municipal wastewater treatment are likely to increase due to metformin's broadening pharmacological efficacy, its widespread use, projected increases in the rates of obesity and diabetes, and the emerging new uses for the compound (2, 16). There is also evidence that metformin and guanylurea may impact some aquatic species (14, 18, 19). In light of these different impacts, guanylurea is considered in many countries to be one of the most prominent emerging water pollutants (20).

While microbial metabolism of metformin is considered to be the major source of guanylurea, it can also derive from other anthropogenic and natural sources. Guanylurea may also accumulate from the microbial degradation of cyanoguanidine (dicyanodiamide), a common fertilizer additive (21, 22). Derivatives of guanylurea are utilized in the manufacture of flame retardants as well as propellants for energetic compounds and munitions (23, 24). Natural products containing the guanylurea moiety have been identified in the red alga *Gymnogongrus flabelliformis*. These compounds include the novel amino acid gigartinine and a guanylureido acid named gongrine (25–27), which are proposed to play a role in nitrogen metabolism (28) and may contribute to faster spring growth for certain marine plants (29).

Given the prevalent use of metformin and frequent detection of guanylurea in aquatic environments, research on the microbial degradation of these compounds is essential to develop biotechnological applications for bioremediation and wastewater treatment. Several studies have recently investigated the biodegradation of metformin and guanylurea by microbial communities isolated from activated sludge (8, 11). In one study not involving metformin, the disappearance of guanylurea was shown to be accompanied by the appearance of guanidine as measured by high-performance liquid chromatography (HPLC) analyses, suggesting guanidine as a potential transformation product (23). These studies examined the microbial breakdown of guanylurea but did not define metabolic pathways or the genes and enzymes mediating breakdown.

The present study describes the biodegradation of guanylurea by a *Pseudomonas mendocina* bacterium isolated, by enrichment, from a wastewater treatment plant. This bacterium utilized guanylurea as a nitrogen source for growth. Genome sequencing and bioinformatic analyses led to the identification of genes involved in the biodegradation of ureide and guanidinium compounds. A new member of the isochorismatase-like hydrolase protein family was shown to catalyze the conversion of guanylurea to guanidine, and the enzyme was characterized physically and kinetically. A mineralization pathway to ammonia and carbon dioxide was demonstrated. Insights obtained here may now be used with wastewater metagenome data to predict the intrinsic capacity for guanylurea biodegradation.

TABLE 1 Comparison of general genome properties of *Pseudomonas mendocina* ymp and *Pseudomonas mendocina* strain GU[a]

General sequencing and genome property	Value	
	Pseudomonas mendocina ymp	*Pseudomonas mendocina* strain GU
Genome coverage (fold)	14	36
Size (Mb)	5.0	5.7
G+C content (%)	64.7	64.3
No. of protein-coding genes	4,704	5,378
Coding regions (% genome)	90.8	91.5
Avg ORF[b] size (bp)	980	975

[a]*P. mendocina* ymp was sequenced by the Joint Genome Institute and strain GU was sequenced as part of the present study.
[b]ORF, open reading frame.

RESULTS

Enrichment and isolation of a pure culture growing on guanylurea. Activated sludge from the Saint Paul, MN, municipal wastewater treatment plant was used as a source of bacteria for enrichment on guanylurea as the sole nitrogen source. After the first five transfers, guanylurea utilization was indicated by a significant increase in optical density in liquid culture and appearance of individual colonies on agar plates containing LB or guanylurea minimal medium. Subsequent transfers and plating of individual colonies led to the isolation of a pure culture with guanylurea-degrading capability as demonstrated by HPLC. No guanylurea was detected in the spent growth medium of the cultures after 24 h of incubation. Control media which were not inoculated did not exhibit significant guanylurea disappearance (<5%). The 16S rRNA sequence analysis identified the bacterium as a *Pseudomonas mendocina*, and it was designated here as strain GU.

Pseudomonas mendocina strain GU was able to utilize guanidine, agmatine, and urea as sole sources of nitrogen for growth, using citrate and acetate as carbon sources (see Table S1 in the supplemental material). The doubling time with guanylurea was 44 min. Doubling times with other nitrogen-rich compounds analogous to guanylurea ranged from 66 to 92 min: agmatine (66 min), guanidine (81 min), and urea (92 min). No growth was observed when biuret, metformin, or cyanoguanidine was used as the sole nitrogen source.

Genome sequencing and analysis of *P. mendocina* strain GU. The strain was subjected to Illumina sequencing with 36-fold coverage. The *P. mendocina* strain GU genome showed a high degree of gene sequence relatedness (see Table S2) and synteny (see Fig. S1) with *P. mendocina* ymp, which was isolated from Yucca Mountain hazardous waste repository (30). Properties of the two genomes are compared in Table 1. Overall, the two genomes shared 98% average nucleotide sequence identity, and 77.6% of the predicted proteins in the genome of *P. mendocina* strain GU shared >95% sequence identity to proteins present in the genome of strain ymp (Table S1). The major difference was the presence of an additional 665 coding sequences in strain GU (12.4% of the genome). Taken together, only 10% of the shared proteins were less than 95% identical.

Identification and purification of a guanylurea-degrading enzyme. Guanylurea degradation genes or enzymes had not previously been identified. In light of this, the genome sequence of *P. mendocina* strain GU was mined for the presence of genes that might encode enzyme classes that act on the guanidine or urea functional groups that, in combination, compose guanylurea. Genes encoding enzymes annotated to be active with the guanidinium compounds arginine and agmatine were identified but, based on the flanking genes, were thought not to be relevant to guanylurea. The organism has genes encoding an active urease, but urease was previously tested for activity with guanylurea and shown to be inactive (31). A gene encoding a protein annotated from BLAST comparisons as "cysteine hydrolase" and "nicotinamidase" was analyzed in more detail. The translated amino acid sequence showed 48% sequence identity to a

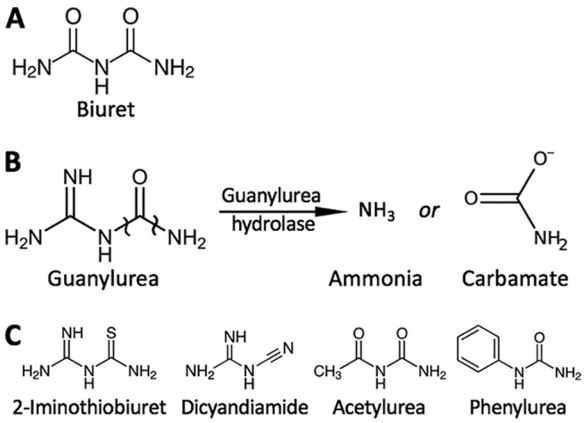

FIG 1 (A to C) Compounds and reaction in the present study.

biuret hydrolase (BiuH) from *Rhizobium leguminosarum* that had been characterized functionally (32). We noted that biuret is structurally analogous to guanylurea, having only an oxygen replacing one of the guanylurea guanidinium nitrogen atoms (Fig. 1A and B). In this context, a synthetic gene encoding the biuret hydrolase homolog (NCBI accession no. MBF8163004.1) was obtained and expressed in *Escherichia coli*, and the His-tagged enzyme was purified in one step to homogeneity via a Ni affinity column. Incubation of the purified enzyme with guanylurea produced 1 mol of ammonia per mol of guanylurea, identifying this enzyme to be capable of degrading guanylurea. No redox cofactors or oxygen was required, indicating that the enzyme was a guanylurea hydrolase.

Characterization of the guanylurea hydrolase enzyme. It was important to examine the kinetics and substrate specificity of the enzyme described above to determine if this enzyme was competent to support significant guanylurea degradation and if that was the major native activity. The purified enzyme was active over a pH range of 5.5 to 8.5, with highest specific activity at pH 8.0. At the pH optimum, the specific activity of purified guanylurea hydrolase with saturating guanylurea was 13 μmol per min per mg (Table 2). The k_{cat}/K_m was higher (3-fold) than for the average enzyme with its cognate substrate, as compiled from a study of thousands of enzymes by Davidi and coworkers (33). The enzyme showed minimal activity on biuret, with 0.06% the specific activity measured on guanylurea. Moreover, no activity ($<$0.01 μmol per min per mg) was detected with acetylurea, dicyandiamide, phenylurea, nitroguanidine, and 2-imino-thiobiuret (Fig. 1C). These data indicate that the major biological function of the enzyme studied here is to release ammonia from guanylurea, allowing *P. mendocina* strain GU to grow on guanylurea.

Elucidating the guanylurea hydrolase reaction product. In addition to ammonia, guanidine was stably produced in incubations with guanylurea hydrolase and guanylurea. This could arise from hydrolytic cleavage of the terminal urea C-N bond or the subterminal N-C bond (Fig. 1B). The former cleavage reaction would produce ammonia

TABLE 2 Biochemical and molecular properties of guanylurea hydrolase

Property	Exptl determination
Subunit mol wt	24.8 kDa
Subunit structure	α_4
Calculated pI	5.5
pH optimum	8.0
Sp act	13 μmol/min per mg
k_{cat}	5.2 s^{-1}
K_m	16 μM
k_{cat}/K_m	3.3×10^5 s^{-1} M^{-1}

and carboxyguanidine, which readily decarboxylates, forming stable guanidine. The subterminal bond cleavage would produce guanidine directly, along with carbamate. Carbamate at neutral pH in water has a half-life of 70 ms (34), rapidly converting to carbon dioxide and ammonia. So, both reactions produce ammonia and guanidine rapidly from unstable intermediates. However, it is now possible to "observe" carboxyguanidine because an enzyme that rapidly converts it to allophanate and ammonia was recently discovered (35). In that previous study, guanidine carboxylase produced highly unstable carboxyguanidine that was rapidly hydrolyzed into a more stable compound, allophanate, via carboxyguanidine deiminase (CgdAB). Allophanate hydrolase was used to convert allophanate to ammonia and carbon dioxide. Here, an analogous experiment was performed by adding the enzymes CgdAB and allophanate hydrolase to GuuH reactions. If carboxyguanidine was formed, the additional enzymes would release an additional three equivalents of ammonia. If guanidine and carbamate were formed, no additional ammonia would be released. None of the enzymes have activity with guanidine.

In two separate experiments, carried out as described in the Materials and Methods, no increase in ammonia was observed in kinetic (short-term incubations) or stoichiometric (long-term incubations) experiments, indicating that guanidine is produced directly. In these experiments, an up to 40-fold excess of coupling enzymes were added, which would have released additional ammonia from carboxyguanidine, if that had been produced by GuuH.

Gene regions of the *P. mendocina* strain GU genome related to guanylurea mineralization. With the observation that guanidine and carbamate are the likely products of the GuuH enzyme, and carbamate that decays spontaneously liberates one ammonia molecule, further ammonia release would require enzymes implicated in guanidine degradation. Guanidine metabolism has only recently been elucidated, and special identifying features of the genes were reported (35). That information was used to aid in bioinformatic analysis of predicted protein-encoding regions in the *P. mendocina* strain GU genome (Fig. 2).

First, the guanylurea hydrolase gene (*guuH*), identified in this study, did not appear to be contiguous to genes encoding enzymes involved in related metabolism that we could discern (Fig. 2A). The only identifiable surrounding genes were ABC transporters of unknown function. A gene region likely to be involved in guanidine metabolism was localized ~400 genes distant (Fig. 2B). The large gene clearly encodes an enzyme including the biotin-binding domain and other regions diagnostic for carboxylases (36). The carboxylase is further identified as a guanidine-metabolizing enzyme by a specific active region demarcated in a previous study (35). Guanidine carboxylases contain an aspartic acid residue in the active site at a position typically occupied by asparagine in fungal and bacterial urea carboxylases (35), and the protein here contained that diagnostic aspartate. Even stronger evidence is provided by cooccurrence of the *cgdAB* genes next to our annotated guanidine carboxylase (Fig. 2B). The *cgdAB* genes are present in ~7,000 bacterial genomes, and 96% of the time, they colocalize with a guanidine carboxylase (35). The CgdA and CgdB proteins were shown previously to form a complex and to transform the product of guanidine carboxylase, carboxyguanidine, to allophanate. Lastly, guanidine metabolism gene expression was shown to be regulated by guanidine riboswitches (37), and these are found directly upstream of the enzyme-encoding genes just described (Fig. 2B).

Another gene region (genes 300 to 302) in the *P. mendocina* strain GU genome encoded an allophanate hydrolase, an adjacent urea carboxylase, and a regulatory protein, respectively (Fig. 2C). The carboxylase protein encoded by gene 301 contained an asparagine instead of aspartate at its active site, a feature consistent with a preference for urea as the substrate undergoing carboxylation (35). Urea carboxylation produces allophanate, and allophanate hydrolase can degrade that to ammonia and carbon dioxide. In the presence of guanylurea, the five genes highlighted in red in Fig. 2 encode four proteins (CgdA and CgdB function as one protein) that constitute a complete pathway for guanylurea that can liberate all four nitrogen atoms as ammonia (Fig. 2D).

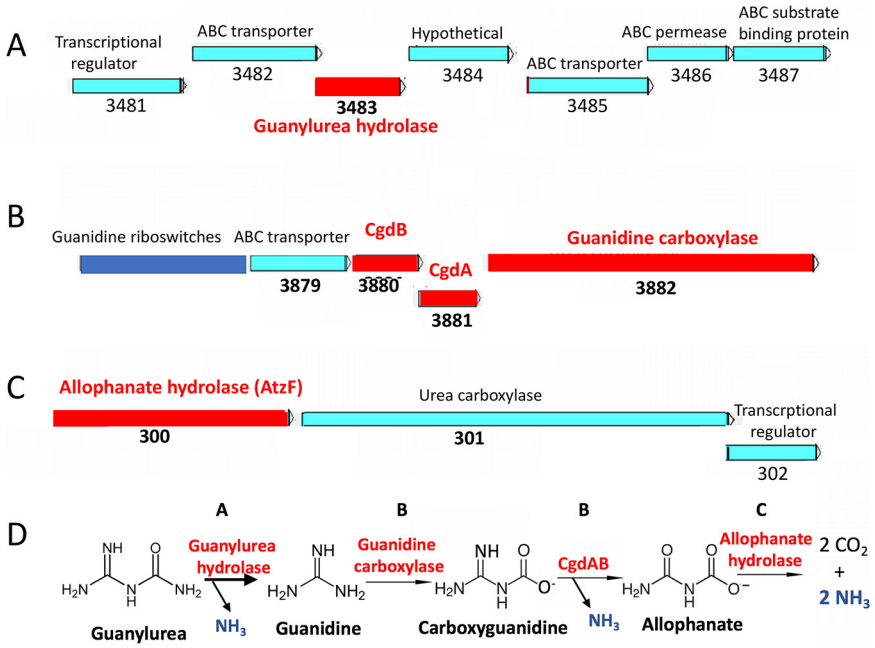

FIG 2 Gene regions identified in *P. mendocina* strain GU and biodegradative pathway. (A) Genes 3481 to 3487; (B) genes 3879 to 3882; (C) genes 300 to 302. (D) Metabolic pathway via enzyme reactions and NH_3 stoichiometry.

In addition to the genomics and bioinformatic inferences described above, there is direct experimental data consistent with the pathway shown in Fig. 2D. First, *P. mendocina* strain GU grows readily on guanidine as a sole nitrogen source. Only one metabolic pathway for guanidine is currently known and that proceeds as shown in Fig. 2, via guanidine carboxylase, CgdAB, and allophanate hydrolase (35), for which genes are present in *P. mendocina* strain GU.

To further test the pathway shown in Fig. 2D experimentally, we carried out ammonia stoichiometry experiments. If all of the relevant genes shown in Fig. 2 are expressed, it is predicted that 4 equivalents of ammonia would be produced for each guanylurea molecule consumed. To test this hypothesis, parallel cultures of *P. mendocina* strain GU were grown with limiting amounts of nitrogen, and then cell densities were determined when growth ceased. As shown in Fig. 3, the growth on 1 mol of guanylurea, containing four nitrogen atom equivalents, was the same as with 4 mol of ammonium ion. For example, separate growth cultures containing 1.92 mM ammonium chloride or 0.48 mM guanylurea each grew to an optical density at 600 nm (OD_{600}) of 0.8. Both contained the same number of nitrogen atoms, equivalent to 1.92 mM ammonia. These data are consistent with guanylurea being completely mineralized to release all the nitrogen atoms contained within the compound. One can draw out a chemically plausible pathway in which guanylurea undergoes a direct deamination reaction to produce biuret, but biuret was negative as a growth substrate and metabolism producing biuret would only yield one nitrogen equivalent, not four as was observed.

Guanylurea hydrolase is a new member of the isochorismatase hydrolase-like protein family. A query of the Pfam database with the GuuH amino acid sequence gave a match to the isochorismatase hydrolase-like (IHL) protein family (PF00857.20) with an E value of $7.1e^{-42}$. GuuH (GH in Fig. 4) consists of 231 amino acids and matched extensively over amino acids 26 to 217 with biuret hydrolase (BH) and triuret hydrolase (TH) (Fig. 4). IHL proteins are sometimes denoted as cysteine hydrolases, and GuuH contains a cysteine, C171, that aligns with a cysteine in BH and TH and found in a highly conserved region (Fig. 4A). X-ray structures have been determined for biuret (38) and triuret hydrolases (39), and those studies have revealed the cysteine aligning

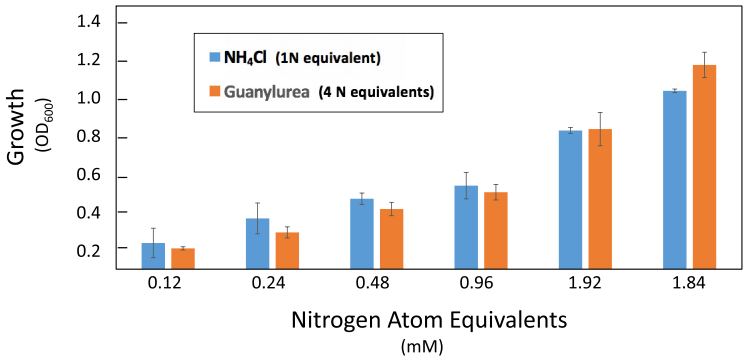

FIG 3 Nitrogen growth comparison by setting molar amounts of nitrogen in ammonium chloride equivalent to guanylurea. Growth was conducted as described in Materials and Methods.

with C171 in GuuH acts as a nucleophile to catalyze initial bond cleavage. The resulting acyl enzyme intermediate further undergoes hydrolysis to complete the reaction. Those structural and mechanistic studies have also revealed that the biuret and triuret hydrolase active sites both contain a D-K-C catalytic triad, of which all the residues reside in GuuH in alignment and in highly conserved regions of the protein overall (Fig. 4A).

One notable difference in the sequences was with a glutamine residue that helps bind substrate in biuret and triuret hydrolases and that was replaced with a glutamate in GuuH, as illustrated in Fig. 4B. X-ray structures for biuret and triuret hydrolases reveal that the glutamine residue hydrogen bonds to the substrate amide group distal to the one reacting at the active site cysteine (38, 39). The change to an aligning glutamate, Glu221, in GuuH is logical, chemically, as the negatively charged glutamate would be expected to bind electrostatically to the positively charged guanidinium group, thus aligning the guanylurea substrate in a similar manner as biuret and triuret hydrolases align their substrates. This suggests that the glutamine-to-glutamate change is key for differentiating GuuH enzymes from biuret and triuret hydrolases.

To test this hypothesis, we mutated the glutamine residue in the biuret hydrolase from *Herbaspirillum* sp. strain BH-1 (Gln212) that corresponds to Glu221 of GuuH and

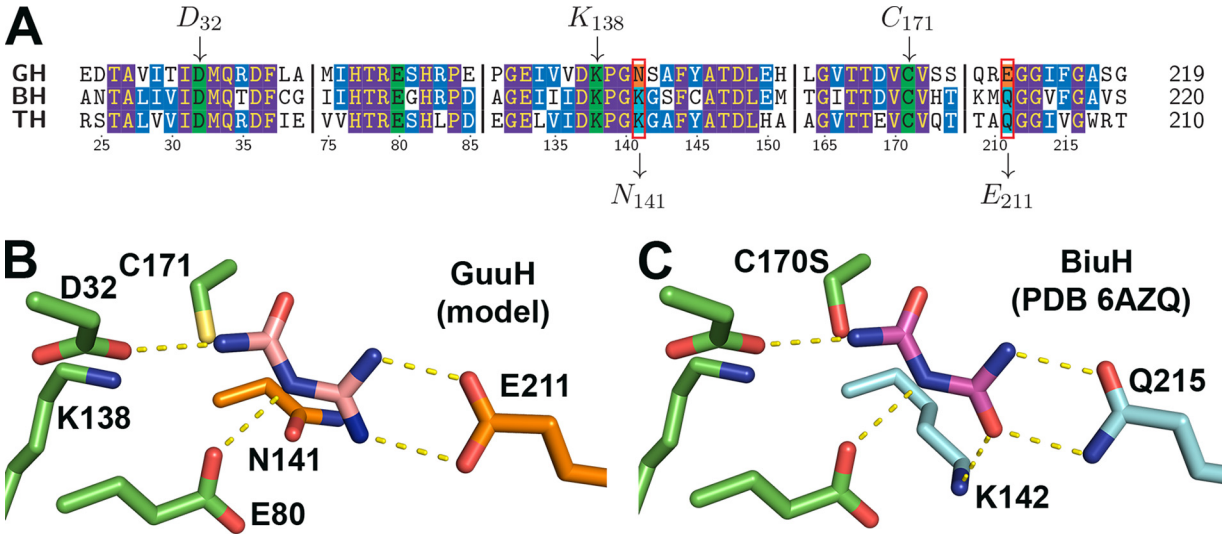

FIG 4 Sequence alignment and structural comparisons of guanylurea hydrolase (GH) with biuret hydrolase (BH) and triuret hydrolase (TH). (A) Sequence alignment was made using NCBI COBALT alignment tool with the BH (PLY61274.1) and TH (PLY61272.1) sequences from *Herbaspirillum* BH-1. (B and C) Key amino acid positions differentiating guanylurea (E211) and biuret (Q215) hydrolases, derived from Protein Data Bank structure 6AZQ. Homology model of GuuH made with BiuH as a template (48% sequence identity). The C170S variant of BiuH is catalytically dead, which allows for cocrystals with biuret.

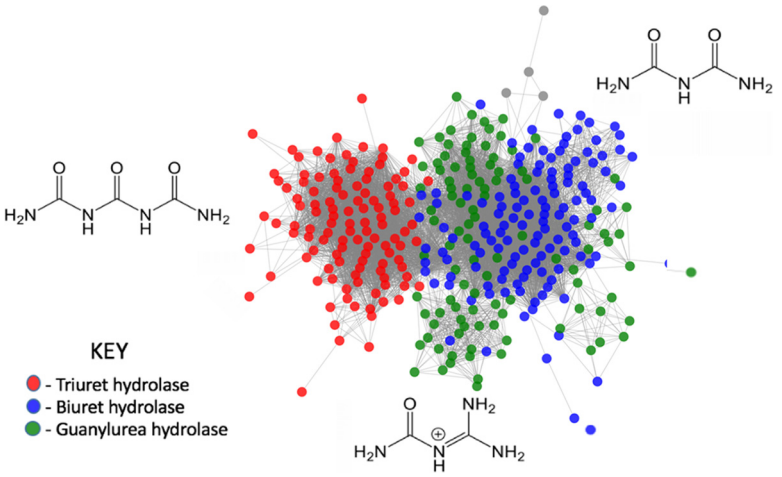

FIG 5 Sequence similarity network (SSN) of 3,700 sequences of IHL proteins determined or predicted to degrade triuret, biuret, or guanylurea. There are >1,900 sequences ranging in identity from 45% to 100%. SSN built using EFI-EST with a cutoff of E−65 and visualized with Cytoscape.

replaced the residue with a glutamate residue. The resulting enzyme, BiuH Q212E, showed nearly 2 orders of magnitude diminished activity with biuret compared to that of the wild type, and guanylurea hydrolysis became the dominating function of the enzyme, with 40% higher activity with guanylurea than with biuret (see Table S3). The wild-type biuret hydrolase showed no detectable activity with guanylurea (Table S3). This result demonstrated that a single point mutation can convert a biuret hydrolase to an enzyme significantly active with guanylurea. Triuret hydrolases have a larger active site, and the glutamine residue is significantly further away from the catalytic cysteine than in GuuH and biuret hydrolases (39). These different properties also allow discrimination between the closely related GuuH enzymes, biuret hydrolases, and triuret hydrolases (Fig. 5).

The defining signatures that identified biuret, triuret, and guanylurea hydrolases (Fig. 4) were used with sequence similarity network (SSN) analysis to look broadly at the interrelationships of the three homologous enzymes with closely aligning sequences pulled from GenBank. The SSN analysis showed the GuuH enzymes to be more closely related to the biuret hydrolases, consistent with the similar sizes of the substrates and their ready interconversion (Fig. 5). The observation that there were several separated lobes of GuuH sequences in the SSN may suggest that different sequence clusters of GuuH enzymes arose independently from biuret hydrolases, consistent with our observation of a single point mutation changing activities. Guanylurea may largely derive from metformin and the fertilizer additive cyanoguanidine, both which are only recently in the environment, perhaps suggesting a recent evolutionary origin of at least some GuuHs.

DISCUSSION

There is increasing focus on the occurrence of human pharmaceuticals in surface and wastewaters, and metformin is often at or near the top of the list with respect to the number of source detections and levels (40). Metformin has a moderate half-life of 5 to 10 days in river simulation studies, with variation related to microbial diversity (41). However, because of metformin's extremely high usage, with 70 million prescriptions annually and gram quantities per daily dose, the compound is continuously introduced into surface waters and wastewater treatment plants. For many anthropogenic chemicals in the environment, levels of stable microbial degradation products often exceed those of the parent compound (42), and this is almost invariably the case with metformin. Guanylurea has long been identified as a relatively persistent and high-level transformation product of metformin (11, 12). The persistent high levels of guanylurea have led to it being labeled as a "dead-end" product of metformin.

While there have been reports of guanylurea biodegradation (11, 12, 43), this report identifies specific genes, enzymes, and a metabolic pathway mediating its metabolism. In the present study, we isolated a bacterium from a wastewater treatment plant that degrades guanylurea to meet its nitrogen needs, sequenced the genome, identified and purified a new guanylurea-hydrolyzing enzyme, elucidated a metabolic pathway for guanylurea mineralization, and identified the evolutionary origins and connectivity of the guanylurea hydrolase to homologous enzymes in the IHL protein family, a part of the cysteine hydrolase superfamily.

As of 9 November 2020, in recorded genomes from NCBI and EMBL databases, GuuH is encoded in less than 0.5% of genomes. The potential rare occurrence of GuuH in the environment and the gene regulation in guanylurea metabolism may play a role in the accumulation of guanylurea in certain environments. Guanidine metabolic genes encoding guanidine carboxylase and carboxyguanidine deiminase can be turned on by a guanidine-sensing riboswitch, which is present in *P. mendocina* strain GU, but there has been no insight into a suppression mechanism of these genes in the presence of guanidine that could be coordinated by broader nitrogen or carbon metabolism, for example (37). The entire regulation of guanylurea metabolic genes, which are encoded in three separate regions of the genome, is complex and will be examined in detail in a future study.

The results presented here have utility in at least two distinct areas. The first is in environmental studies, specifically, where the fates of metformin, cyanoguanidine (44), and guanylurea are being examined. The results here present a roadmap for identifying specific bacteria, genes, and metabolic enzymes that would be present in a particular environment of interest. For example, wastewater metagenomic data (45) may now be culled to look for the presence of these genetic capacities. The second outgrowth of the data would be in medical studies. Metformin prescription rates are expected to rise given its efficacy for treating type 2 diabetes, obesity, and now, perhaps, COVID-19 (7). Metformin is not known to be metabolized by human drug-metabolizing enzymes, but it is known to impact the bacteria in human intestines (46). Indeed, several studies indicate that the human gut microbiome plays a significant role in modulating metformin's therapeutic effects, but the mechanisms of that modulation are currently obscure (47). In light of the overlapping environmental and medical implications, the metabolism of metformin, which largely appears to occur via guanylurea, has heightened importance.

It is intriguing to consider that new GuuH enzymes may be arising in recent evolutionary time to handle new anthropogenic chemical inputs from the expanding usage of metformin. Biuret and triuret hydrolases appear to be ancient enzymes that have diverged with the taxonomy of the bacteria that harbor them (39, 48). Triuret hydrolases have diverged significantly from biuret hydrolases, a phenomenon clearly indicated by the visual separation on the sequence similarity network shown in Fig. 5. In contrast, the enzymes identified by sequence signatures as GuuH are interspersed and emerging from several regions of the biuret hydrolase enzyme cluster, as shown in Fig. 5. One explanation for this would be that GuuH activities have arisen multiple times from biuret hydrolase precursors. Given that a single mutation can impart significant guanylurea hydrolase activity upon a biuret hydrolase, it is plausible that recent evolution is occurring in different global waters as metformin input increases.

There are other precedents for recent evolution of biodegradative enzymes in response to new anthropogenic environmental inputs. For example, *trans*-3-chloroacrylate dehalogenase from *Pseudomonas cichorii* 170 that degrades the nematicide 1,3-dichloropropene was thought to have arisen in recent evolutionary times from 4-oxalocrotonate tautomerase (49, 50). A similar observation has been made with anthropogenic *s*-triazine compounds, such as the herbicide atrazine, in which atrazine chlorohydrolases arose independently from divergent members of the amidohydrolase protein superfamily (51, 52). Moreover, the fate of anthropogenic chemicals and their metabolites in the environment has been observed to change in recent times as the result of

microbial enzyme evolution (53). Given that GuuH enzymes can readily arise from a biuret hydrolase via simple mutation(s), and the increasing environmental prevalence of compounds giving rise to guanylurea, we expect that guanylurea will increasingly lose its designation as a "dead-end" metabolite.

MATERIALS AND METHODS

Enrichment cultures and isolation of guanylurea-degrading bacteria. The bacterial *Pseudomonas mendocina* strain GU was isolated from a sample of activated sludge collected at the metropolitan wastewater treatment plant in Saint Paul, MN. Isolation was achieved by enrichment culture with citrate-acetate medium and 1 g of sludge per 50 ml of minimal medium as the inoculum. The minimal medium contained the following per liter of deionized water: 5.45 g K_2HPO_4, 0.2 g $MgSO_4 \cdot 7H_2O$, 0.1 g NaCl, 1.5 g 20 mM sodium acetate, and 20 mM sodium citrate (54). Guanylurea (1 mM) was then added as the sole nitrogen source. Enrichments and isolates were grown at 30°C in a shaking incubator at 200 to 225 rpm. Cultures were transferred in 10-fold dilutions into fresh medium every 7 days. Individual isolates were obtained by plating 10-fold serial dilutions of the enrichments on selective guanylurea plates, transferred to Luria-Bertani (LB) plates, and then isolated by streaking on LB and minimal medium plus guanylurea plates until pure.

Growth studies. Growth studies were conducted in triplicates in citrate-acetate medium containing 1 mM each of their respective nitrogen source: guanylurea, biuret, guanidine, urea, or metformin. Nitrogen-free citrate-acetate medium served as a negative control. Citrate-acetate medium containing 6 mM ammonium chloride (NH_4Cl) served as a positive control. Cell growth was monitored spectrophotometrically at 600 nm initially at 12- to 24-h intervals. Cultures with short lag phases were monitored every 4 to 6 h.

DNA extraction and PCR testing for taxonomic identification. Genomic DNA was purified utilizing a Qiagen DNeasy blood and tissue kit (Qiagen, Valencia, CA) and Promega Wizard genomic DNA purification kit (Promega, Madison, WI). PCR amplification for taxonomic identification of bacterial strains was performed with universal 16S primers, 530F (5′-GTGCCAGCMGCCGCGG-3′) and 1492R (5′-GGTTACCTTGTTACGACTT-3′), using Q5 high-fidelity polymerase (New England BioLabs, Ipswich, MA). Amplification of the 1.4-kb DNA 16S rRNA fragment was achieved using the following conditions: 98°C for 2 min, and then 35 cycles consisting of 95°C for 1 min, 60°C for 30 s, and 72°C for 1 min; a final extension of the PCR product was performed at 72°C for 5 min. All PCRs were carried out using a concentration of 0.5 μM for each primer. Amplification products were purified using the QIAquick DNA extraction kit and sequenced (Functional Biosciences, WI, USA) to determine the identity of the microbial isolate.

HPLC analysis. HPLC testing was conducted with a Waters IC-Pak anion HC column, 4.6 by 150 mm. Isocratic mobile phase consisted of a 5 μM KPO_4 buffer at pH 8.0, and the flow rate was 0.5 ml/min. Eluents were monitored at 194 nm. Standards were in 125 mM KPO_4 buffer, pH 8.0. Spent medium was analyzed by HPLC after cells were grown in citrate-acetate medium containing 1 mM guanylurea for 24 h. Cells were centrifuged at 3,000 $\times$ *g* for 15 min, and supernatant was then collected and filter sterilized through a 0.2-μm filter. Controls included sterilized N-free medium and 1 mM guanylurea solution. Enzyme was prepared at a concentration of 1 μg/ml in 125 mM KPO_4 buffer, pH 8.0, with 1 mM guanylurea. Samples were incubated either overnight at room temperature or for 30 min and boiled for 2 min to inactivate enzyme.

Genome sequencing and analysis. Total genomic DNA from microbial isolates was sequenced using a Roche GS 454 FLX system and standard LR 70 chemistry. Illumina Nextera XT library preparation and sequencing (on a MiSeq with V3 chemistry and 300-bp paired-end reads) services were provided by the University of Minnesota Biomedical Genomics Center (BMGC, Saint Paul, MN, USA). Adaptors and low-quality bases were trimmed from raw reads with trimmomatic v 0.36. *De novo* assembly was performed using SPAdes v 3.13.0 (55). Initial genome annotation was performed with prokka v 1.12 (56). Sequence similarity networks were made using the enzyme function initiative-enzyme similarity tool (EFI-EST) (University of Illinois at Urbana-Champaign), retrieving 10,000 sequences related to GuuH (57). The network was visualized in Cytoscape, and the clusters of guanylurea hydrolase, biuret hydrolase, and triuret hydrolase were identified as presented in Fig. 5 (58).

Protein expression and chromatography. The putative GuuH gene (NCBI accession no. MBF8163004.1) was codon optimized for *E. coli* and synthesized by Integrated DNA Technologies (Coralville, IA). The gene was cloned into a pET28b+ vector with Gibson assembly master mix (New England BioLabs) using NdeI and HindIII restriction sites with an N-terminal 6×His tag and transformed into BL21-DE3 *E. coli* cells (New England BioLabs). Site-directed mutants of the biuret hydrolase from *Herbaspirillum* sp. BH-1 (NCBI accession no. PLY61274.1) and *guuH* were made using the Q5 site-directed mutagenesis kit from New England BioLabs. The *guuH* gene was expressed by growing cells in lysogeny broth (LB) medium with 50 μg/ml kanamycin at 37°C and 200 rpm to an OD_{600} of 0.6 in a shake flask. The culture was cooled to 14°C and induced with 1 mM isopropyl β-D-1-thiogalactopyranoside (IPTG) and, with the same agitation, incubated for 20 h. Induced cells were harvested at 4,000 $\times$ *g* and resuspended in lysis buffer (20 mM phosphate, 200 mM NaCl, pH 7.4). Cells were lysed with 3 passes in a French press at 10,000 lb/in^2. The cells were centrifuged for 90 min at 19,000 $\times$ *g*, and the supernatant was passed through 0.2-μm filter prior to loading into a GE Life Sciences AKTA fast liquid protein chromatography (FPLC) system for injection onto a GE Life Sciences HisTrap HP 5-ml column. After washing to limit nonspecific protein binding, GuuH was eluted with a linear gradient from 0.1 M to 0.25 M imidazole in lysis buffer over 10 column volumes with flow rate set at 2 ml/min, and fractions

were collected. To determine the oligomeric state of GuuH, gel filtration was performed using a GE Healthcare HiLoad 16/600 Superdex 200-pg column. The column was equilibrated with 50 mM Tris-200 mM sodium chloride at pH 8, and the sample was injected onto the column and washed with 1 column volume at 1 ml/min flow rate, with GuuH eluted as a homotetramer at ~96 kDa.

Enzyme assays. Enzyme activity was measured by detection of ammonia release using the Berthelot reaction as previously described (59). Experiments were performed at room temperature in 125 mM sodium phosphate dibasic buffer at pH 8. Specific activity at 25°C was determined at the pH optimum for the enzyme using the appropriate buffer (acetate, pH 5.5 to 6.5; phosphate, pH 7.0 to 8.0; borate, pH 8.5 to 10.5) with 1 mM guanylurea.

CgdAB from *Pseudomonas syringae*, a heterodimeric enzyme (NCBI accession no. WP_005764729.1 and WP_005764727.1, respectively), and allophanate hydrolase from *Pseudomonas* sp. strain ADP (NCBI accession no. WP_011117193.1) were employed in coupled enzyme assays to determine if carboxyguanidine is formed during GuuH hydrolysis of guanylurea (35). The CgdAB protein was a gift from Martin St. Maurice of Marquette University, and it was shown to be active in a coupled assay with guanidine carboxylase with guanidine as the substrate. Enzyme kinetic assays were performed in a 125 mM sodium phosphate dibasic buffer solution, pH 8, with 1 mM guanylurea as the substrate. To initiate the reaction, GuuH was added to a final assay concentration of 0.27 μg/ml. CgdAB was added to a final assay concentration of 15.6 μg/ml and AtzF protein to a final concentration of 7.38 μg/ml. Ammonia release was measured utilizing the Berthelot assay (59). The assay was measured in a Beckman Coulter DU 640 UV-visible (UV-Vis) spectrophotometer.

A coupled enzyme assay to determine stoichiometries of the guanylurea and ammonium liberated utilized GuuH, AtzF, and CgdAB proteins. The reactions were performed overnight in a solution containing 50 μM guanylurea in 125 mM sodium phosphate, pH 8. Enzyme concentrations were 60 μg/ml GuuH, 15.6 μg/ml CgdAB, and 7.38 μg/ml AtzF. Reaction mixtures were incubated at 20°C overnight, and stoichiometries were determined by ammonia release utilizing the Berthelot reaction as described previously.

Data availability. Genome sequences for *Pseudomonas mendocina* strain GU are available in GenBank at BioProject accession PRJNA675777 or BioSample accession SAMN16722328.

SUPPLEMENTAL MATERIAL

Supplemental material is available online only.

SUPPLEMENTAL FILE 1, PDF file, 0.3 MB.

ACKNOWLEDGMENTS

We acknowledge the kind gift of CgdAB enzyme from Martin St. Maurice of Marquette University. We thank Sara Palacios for help with the initial guanylurea enrichment cultures.

This work was funded by the National Institute of Food and Agriculture, Agricultural and Food Research Initiative Competitive Program, Ecosystem Services and Agro-Ecosystem Management, grant no. 2019-67019-29403 to L.P.W. and B.M.-V. and National Institutes of Health Biotechnology training grant (5T32GM008347-27) for L.J.T.

REFERENCES

1. Gong L, Goswami S, Giacomini KM, Altman RB, Klein TE. 2012. Metformin pathways: pharmacokinetics and pharmacodynamics. Pharmacogenet Genomics 22:820–827. https://doi.org/10.1097/FPC.0b013e3283559b22.
2. Briones RM, Zhuang WQ, Sarmah AK. 2018. Biodegradation of metformin and guanylurea by aerobic cultures enriched from sludge. Environ Pollut 243:255–262. https://doi.org/10.1016/j.envpol.2018.08.075.
3. Scheen AJ. 2020. Metformin and COVID-19: from cellular mechanisms to reduced mortality, diabetes and metabolism. Diabetes Metab 46:423–426. https://doi.org/10.1016/j.diabet.2020.07.006.
4. Scheurer M, Sacher F, Brauch H-J. 2009. Occurrence of the antidiabetic drug metformin in sewage and surface waters in Germany. J Environ Monit 11:1608–1613. https://doi.org/10.1039/b909311g.
5. Novelle MG, Ali A, Diéguez C, Bernier M, de Cabo R. 2016. Metformin: a hopeful promise in aging research. Cold Spring Harb Perspect Med 6:a025932. https://doi.org/10.1101/cshperspect.a025932.
6. Amin S, Lux A, O'Callaghan F. 2019. The journey of metformin from glycaemic control to mTOR inhibition and the suppression of tumour growth. Br J Clin Pharmacol 85:37–46. https://doi.org/10.1111/bcp.13780.
7. Bramante C, Ingraham NE, Murray TA, Marmor S, Hovertsen S, Gronski J, McNeil C, Feng R, Guzman G, Abdelwahab N, King S, Meehan T, Pendleton KM, Benson B, Vojta D, Tignanelli CJ. 28 June 2020. Observational study of metformin and risk of mortality in patients hospitalized with Covid-19. medRxiv https://doi.org/10.1101/2020.06.19.20135095.
8. Trautwein C, Kümmerer K. 2011. Incomplete aerobic degradation of the antidiabetic drug metformin and identification of the bacterial dead-end transformation product guanylurea. Chemosphere 85:765–773. https://doi.org/10.1016/j.chemosphere.2011.06.057.
9. Bradley PM, Journey CA, Button DT, Carlisle DM, Clark JM, Mahler BJ, Nakagaki N, Qi SL, Waite IR, VanMetre PC. 2016. Metformin and other pharmaceuticals widespread in wadeable streams of the southeastern United States. Environ Sci Technol Lett 3:243–249. https://doi.org/10.1021/acs.estlett.6b00170.
10. Bradley PM, Battaglin WA, Clark JM, Henning FP, Hladik ML, Iwanowicz LR, Journey CA, Riley JW, Romanok KM. 2017. Widespread occurrence and potential for biodegradation of bioactive contaminants in Congaree National Park, USA. Environ Toxicol Chem 36:3045–3056. https://doi.org/10.1002/etc.3873.
11. Briones RM, Sarmah AK, Padhye LP. 2016. A global perspective on the use, occurrence, fate and effects of antidiabetic drug metformin in natural and engineered ecosystems. Environ Pollut 219:1007–1020. https://doi.org/10.1016/j.envpol.2016.07.040.
12. Scheurer M, Michel A, Brauch HJ, Ruck W, Sacher F. 2012. Occurrence and fate of the antidiabetic drug metformin and its metabolite guanylurea in the environment and during drinking water treatment. Water Res 46:4790–4802. https://doi.org/10.1016/j.watres.2012.06.019.
13. Tao Y, Chen B, Zhang B, Zhu Z, Cai Q. 2018. Occurrence, impact, analysis and treatment of metformin and guanylurea in coastal aquatic

environments of Canada, USA and Europe. Adv Mar Biol 81:23–58. https://doi.org/10.1016/bs.amb.2018.09.005.
14. Ghoshdastidar AJ, Fox S, Tong AZ. 2015. The presence of the top prescribed pharmaceuticals in treated sewage effluents and receiving waters in southwest Nova Scotia, Canada. Environ Sci Pollut Res Int 22:689–700. https://doi.org/10.1007/s11356-014-3400-z.
15. Blair BD, Crago JP, Hedman CJ, Treguer RJF, Magruder C, Royer LS, Klaper RD. 2013. Evaluation of a model for the removal of pharmaceuticals, personal care products, and hormones from wastewater. Sci Total Environ 444:515–521. https://doi.org/10.1016/j.scitotenv.2012.11.103.
16. Oosterhuis M, Sacher F, Ter Laak TL. 2013. Prediction of concentration levels of metformin and other high consumption pharmaceuticals in wastewater and regional surface water based on sales data. Sci Total Environ 442:380–388. https://doi.org/10.1016/j.scitotenv.2012.10.046.
17. Piai L, Blokland M, van der Wal A, Langenhoff A. 2020. Biodegradation and adsorption of micropollutants by biological activated carbon from a drinking water production plant. J Hazard Mater 388:122028. https://doi.org/10.1016/j.jhazmat.2020.122028.
18. Niemuth NJ, Klaper RD. 2015. Emerging wastewater contaminant metformin causes intersex and reduced fecundity in fish. Chemosphere 135:38–45. https://doi.org/10.1016/j.chemosphere.2015.03.060.
19. Straub JO, Caldwell DJ, Davidson T, D'Aco V, Kappler K, Robinson PF, Simon-Hettich B, Tell J. 2019. Environmental risk assessment of metformin and its transformation product guanylurea. I. Environmental fate. Chemosphere 216:844–854. https://doi.org/10.1016/j.chemosphere.2018.10.036.
20. Meador JP, Yeh A, Young G, Gallagher EP. 2016. Contaminants of emerging concern in a large temperate estuary. Environ Pollut 213:254–267. https://doi.org/10.1016/j.envpol.2016.01.088.
21. Waterhouse H, Wade J, Horwath WR, Burger M. 2017. Effects of positively charged dicyandiamide and nitrogen fertilizer sources on nitrous oxide emissions in irrigated corn. J Environ Qual 46:1123–1130. https://doi.org/10.2134/jeq2017.01.0033.
22. Cassman NA, Soares JR, Pijl A, Lourenço KS, van Veen JA, Cantarella H, Kuramae EE. 2019. Nitrification inhibitors effectively target N_2O-producing *Nitrosospira* spp. in tropical soil. Environ Microbiol 21:1241–1254. https://doi.org/10.1111/1462-2920.14557.
23. Perreault NN, Halasz A, Thiboutot S, Ampleman G, Hawari J. 2013. Joint photomicrobial process for the degradation of the insensitive munition *N*-guanylurea-dinitramide. Environ Sci Technol 47:5193–5198. https://doi.org/10.1021/es4006652.
24. Xiao Z, Liu S, Zhang Z, Mai C, Xie Y, Wang Q. 2018. Fire retardancy of an aqueous, intumescent, and translucent wood varnish based on guanylurea phosphate and melamine-urea-formaldehyde resin. Prog Org Coat 121:64–72. https://doi.org/10.1016/j.porgcoat.2018.04.015.
25. Ito K, Hashimoto Y. 1966. Gigartinine: a new amino-acid in red algae. Nature 211:417. https://doi.org/10.1038/211417a0.
26. Ito K, Miyazawa K, Hashimoto Y. 1966. Distribution of gongrine and gigartinine in marine algae. J Jpn Fish Soc 32:727–729. https://doi.org/10.2331/suisan.32.727.
27. Ito K, Hashimoto Y. 1965. Occurrence of γ-(guanylureido)butyric acid in a red alga, *Gymnogongrus flabelliformis*. Agric Biol Chem 29:832–835. https://doi.org/10.1271/bbb1961.29.832.
28. Takagui M. 1970. Low molecular nitrogen compounds of marine algae. Bull Fish Sci 21:227–233.
29. Laycock MV, Craigie JS. 1977. The occurrence and seasonal variation of gigartinine and L-citrullinyl-L-arginine in *Chondus crispus* Stackh. Can J Biochem 55:27–30. https://doi.org/10.1139/o77-004.
30. Awaya JD, DuBois JL. 2008. Identification, isolation, and analysis of a gene cluster involved in iron acquisition by *Pseudomonas mendocina* ymp. Biometals 21:353–366. https://doi.org/10.1007/s10534-007-9124-5.
31. Deasy CL. 1946. Specificity of the action of urease. J Am Chem Soc 68:1664–1665. https://doi.org/10.1021/ja01212a506.
32. Cameron SM, Durchschein K, Richman JE, Sadowsky MJ, Wackett LP. 2011. A new family of biuret hydrolases involved in *s*-triazine ring metabolism. ACS Catal 2011:1075–1082. https://doi.org/10.1021/cs200295n.
33. Davidi D, Longo LM, Jabłońska J, Milo R, Tawfik DS. 2018. A bird's-eye view of enzyme evolution: chemical, physicochemical, and physiological considerations. Chem Rev 118:8786–8797. https://doi.org/10.1021/acs.chemrev.8b00039.
34. Wang TT, Bishop SH, Himoe A. 1972. Detection of carbamate as a product of the carbamate kinase-catalyzed reaction by stopped flow spectrophotometry. J Biol Chem 247:4437–4440. https://doi.org/10.1016/S0021-9258(19)45003-5.
35. Schneider N, Tassoulas LJ, Laseke A, Zeng D, Reiter N, Wackett LP, St Maurice M. 2020. Solving the conundrum: widespread proteins annotated for urea metabolism in bacteria are carboxyguanidine deiminases mediating nitrogen assimilation from guanidine. Biochemistry 59:3258–3270. https://doi.org/10.1021/acs.biochem.0c00537.
36. Liu Y, Budelier MM, Stine K, St Maurice M. 2018. Allosteric regulation alters carrier domain translocation in pyruvate carboxylase. Nat Commun 9:1384. https://doi.org/10.1038/s41467-018-03814-8.
37. Nelson JW, Atilho RM, Sherlock ME, Stockbridge RB, Breaker RR. 2017. Metabolism of free guanidine in bacteria Is regulated by a widespread riboswitch class. Mol Cell 65:220–230. https://doi.org/10.1016/j.molcel.2016.11.019.
38. Esquirol L, Peat TS, Wilding M, Lucent D, French NG, Hartley CJ, Newman J, Scott C. 2018. Structural and biochemical characterization of the biuret hydrolase (BiuH) from the cyanuric acid catabolism pathway of *Rhizobium leguminasorum* bv. viciae 3841. PLoS One 13:e0192736. https://doi.org/10.1371/journal.pone.0192736.
39. Tassoulas LJ, Elias M, Wackett LP. 10 November 2020. Discovery of an ultra-specific triuret hydrolase (TrtA) illuminates the triuret biodegradation pathway. J Biol Chem https://doi.org/10.1074/jbc.RA120.015631.
40. Bradley PM, Journey CA, Button DT, Carlisle DM, Huffman BJ, Qi SL, Romanok KM, Van Metre PC. 2020. Multi-region assessment of pharmaceutical exposures and predicted effects in USA wadeable urban-gradient streams. PLoS One 15:e0228214. https://doi.org/10.1371/journal.pone.0228214.
41. Posselt M, Mechelke J, Rutere C, Coll C, Jaeger A, Raza M, Meinikmann K, Krause S, Sobek A, Lewandowski J, Horn MA, Hollender J, Benskin JP. 2020. Bacterial diversity controls transformation of wastewater-derived organic contaminants in river-simulating flumes. Environ Sci Technol 54:5467–5479. https://doi.org/10.1021/acs.est.9b06928.
42. Boxall AB, Sinclair CJ, Fenner K, Kolpin D, Maund SJ. 2004. When synthetic chemicals degrade in the environment. Environ Sci Technol 38:368A–-375A. https://doi.org/10.1021/es040624v.
43. Trautwein C, Berset JD, Wolschke H, Kümmerer K. 2014. Occurrence of the antidiabetic drug metformin and Its ultimate transformation product guanylurea in several compartments of the aquatic cycle. Environ Int 70:203–212. https://doi.org/10.1016/j.envint.2014.05.008.
44. Ning J, Ai S, Cui L. 2018. Dicyandiamide has more inhibitory activities on nitrification than thiosulfate. PLoS One 13:e0200598. https://doi.org/10.1371/journal.pone.0200598.
45. Wu L, Ning D, Zhang B, Li Y, Zhang P, Shan X, Zhang Q, Brown MR, Li Z, Van Nostrand JD, Ling F, Xiao N, Zhang Y, Vierheilig J, Wells GF, Yang Y, Deng Y, Tu Q, Wang A, Global Water Microbiome Consortium, Zhang T, He Z, Keller J, Nielsen PH, Alvarez PJJ, Criddle CS, Wagner M, Tiedje JM, He Q, Curtis TP, Stahl DA, Alvarez-Cohen L, Rittmann BE, Wen X, Zhou J. 2019. Global diversity and biogeography of bacterial communities in wastewater treatment plants. Nat Microbiol 4:1183–1195. https://doi.org/10.1038/s41564-019-0426-5.
46. Wu B, Chen M, Gao Y, Hu J, Liu M, Zhang W, Huang W. 2019. *In vivo* pharmacodynamics and pharmacokinetic effects of metformin mediated by the gut microbiota in rats. Life Sci 226:185–192. https://doi.org/10.1016/j.lfs.2019.04.009.
47. Vich Vila A, Collij V, Sanna S, Sinha T, Imhann F, Bourgonje AR, Mujagic Z, Jonkers DMAE, Masclee AAM, Fu J, Kurilshikov A, Wijmenga C, Zhernakova A, Weersma RK. 2020. Impact of commonly used drugs on the composition and metabolic function of the gut microbiota. Nat Commun 11:362. https://doi.org/10.1038/s41467-019-14177-z.
48. Robinson SL, Badalamenti JP, Dodge AG, Tassoulas LJ, Wackett LP. 2018. Microbial biodegradation of biuret: defining biuret hydrolases within the isochorismatase superfamily. Environ Microbiol 20:2099–2111. https://doi.org/10.1111/1462-2920.14094.
49. Poelarends GJ, Whitman CP. 2004. Evolution of enzymatic activity in the tautomerase superfamily: mechanistic and structural studies of the 1,3-dichloropropene catabolic enzymes. Bioorg Chem 32:376–392. https://doi.org/10.1016/j.bioorg.2004.05.006.
50. Poelarends GJ, Almrud JJ, Serrano H, Darty JE, Johnson WH, Hackert ML, Whitman CP. 2006. Evolution of enzymatic activity in the tautomerase superfamily: mechanistic and structural consequences of the L8R mutation in 4-oxalocrotonate tautomerase. Biochemistry 45:7700–7708. https://doi.org/10.1021/bi0600603.
51. Seffernick JL, Wackett LP. 2001. Rapid evolution of bacterial catabolic enzymes: a case study with atrazine chlorohydrolase. Biochemistry 40:12747–12753. https://doi.org/10.1021/bi011293r.
52. Shapir N, Mongodin EF, Sadowsky MJ, Daugherty SC, Nelson KE, Wackett LP. 2007. Evolution of catabolic pathways: genomic insights into microbial *s*-triazine metabolism. J Bacteriol 189:674–682. https://doi.org/10.1128/JB.01257-06.

53. Wackett LP, Robinson SL. 2020. The ever-expanding limits of enzyme catalysis and biodegradation: polyaromatic, polychlorinated, polyfluorinated, and polymeric compounds. Biochem J 477:2875–2891. https://doi.org/10.1042/BCJ20190720.
54. Mandelbaum RT, Wackett LP, Allan DL. 1993. Mineralization of the *s*-triazine ring of atrazine by stable bacterial mixed cultures. Appl Environ Microbiol 59:1695–1701. https://doi.org/10.1128/AEM.59.6.1695-1701.1993.
55. Anonymous. 2018. SPAdes v 3.13.0 manual. http://home.cc.umanitoba.ca/~psgendb/doc/spades/manual.html.
56. Seemann T. 2014. prokka: rapid prokaryotic genome annotation. Bioinformatics 30:2068–2069. https://doi.org/10.1093/bioinformatics/btu153.
57. Gerlt JA, Bouvier JT, Davidson DB, Imker HJ, Sadkhin B, Slater DR, Whalen KL. 2015. Enzyme function initiative-enzyme similarity tool (EFI-EST): a web tool for generating protein sequence similarity networks. Biochim Biophys Acta 1854:1019–1037. https://doi.org/10.1016/j.bbapap.2015.04.015.
58. Shannon P, Markiel A, Ozier O, Baliga NS, Wang JT, Ramage D, Amin N, Schwikowski B, Ideker T. 2003. Cytoscape: a software environment for integrated models of biomolecular interaction networks. Genome Res 13:2498–2504. https://doi.org/10.1101/gr.1239303.
59. Weatherburn MW. 1967. Phenol-hypochlorite reaction for determination of ammonia. Anal Chem 39:971–974. https://doi.org/10.1021/ac60252a045.